Detecting subsurface objects and identifying voids possibilities using the backscatter analysis of surface wave (BASW) method

Julian Ivanov, Richard D. Miller, Daniel Z. Feigenbaum, and Shelby L. Peterie, Kansas Geological Survey*

Summary

We used a multichannel analysis of surface waves approach to study the ability to detect and, in some instances differentiate, subsurface objects from scattered seismic energy. In addition to the conventional backscatter analysis of surface waves (BASW) approach, we used instantaneous amplitudes as an input to the BASW (IA-BASW) to obtain different imaging information. Synthetic seismic data sets models suggest that the IA-BASW technique results in different backscatter patterns for voids and boulders. Thus, this method could increase/decrease the likelihood an observed scatter is from a void. Tests on real-world data from a site with a small, shallow tunnel with a known location show an enhanced seismic tunnel signature relative to other, most likely geology related, backscatters that could possibly be misinterpreted as voids. In such a manner, the IA-BASW technique can be considered an enhancement to the BASW method that may be used to detect and discriminate subsurface anomalies.

Introduction

Analysis of energy from scattered surface waves can be used to obtain information about the heterogeneities in the shallow subsurface (Snieder, 1986; Blonk and Herman, 1994; Park et al., 1998; Herman et al., 2000; Grandjean and Leparoux, 2004; Nasseri-Moghaddam et al., 2007; Luke and Calderón-Macías, 2008). The backscatter analysis of surface wave (BASW) the amplitudes of the surface wave radiating back (toward the source location) from a subsurface heterogeneity (Sloan et al., 2010). BASW has been used to map abandoned mines (Ivanov et al., 2016), been applied in a multi-method approach to detect clandestine tunnels (Sloan et al., 2015), and served as a foundation for the development of more advanced imaging techniques (Schwenk et al., 2016).

The BASW method is applied by performing the following steps. An *f-k* filter is applied to raw seismic shot records to attenuate the amplitudes of the dominant, forward propagating (i.e., from source to receivers) surface-waves, resulting in the enhancement of back scattered (i.e., from a possible scatter object, if such exists, to the source) surface-wave energy. Next, a frequency-velocity linear moveout (FV-LMO) (Park et al., 2002) correction is applied to shot records using phase-velocities estimated from MASW dispersion-curve images. As a result, forward propagating energy is moved to t = 0 and backscatter energy dominates the seismic records. Traces with the same receiver location are summed, constructively stacking backscatter energy on the resulting 2D backscatter section (Sloan et al., 2010. Displaying these data in instantaneous amplitudes can be a preferred approach for interpreting the final results (Sloan et al., 2015). However, at its current stage of development the BASW method cannot be used to distinguish different types of scattering objects, such as voids, boulders or other heterogeneities. Analysis of both synthetic and real seismic data using the instantaneous amplitudes BASW (IA-BASW), where the instantaneous amplitudes serve as the input for BASW, provided images with different signature responses from voids and boulders.

Synthetic Seismic Model

Two synthetic seismic data sets were calculated using FFDM, a proprietary software from the Kansas Geological Survey for seismic-data modeling, specifically tuned for the estimation of surface-wave propagation (Zeng et al., 2011). Background seismic model parameters were selected using a 1-layer model (Table 1), which was 450 m wide and 45 m deep.

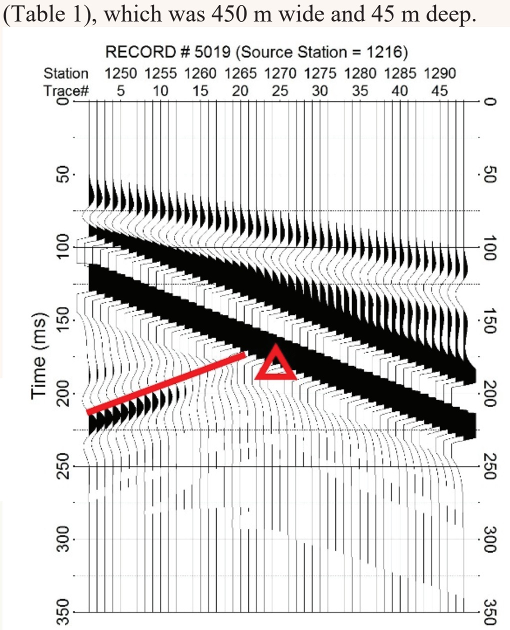

Figure 1. The synthetic seismic shot gather 5019 for source stationed at station 1216 (field layout shown on Figure 2) with backscatters (along the red line) originating from the void located at station 1270.

One of the models contained a void and the other a boulder with velocities two times greater than the background (Table 2). Thirty-two synthetic shot records were calculated from each model using a 25-Hz Ricker wavelet located 30 m away from the nearest receiver. Both anomalies were 1.6 x 1.6 m and located at 10 m depth. Forty-eight vertical receivers were spaced at 1 m, intervals (Figure 1). Data were acquired with a roll-along style of survey with source and receivers advancing at 2 m increments.

Table 1. The single-layer model parameters used for the calculation of synthetic seismic data.

Layer	V_s(m/s)	V_p(m/s)	Dens. (g/m^3)
1	500	1000	1.8

Table 2. The boulder parameters used for the calculation of synthetic seismic data.

Void	V_s(m/s)	V_p(m/s)	Dens. (g/m^3)
1	1000	2000	2.6

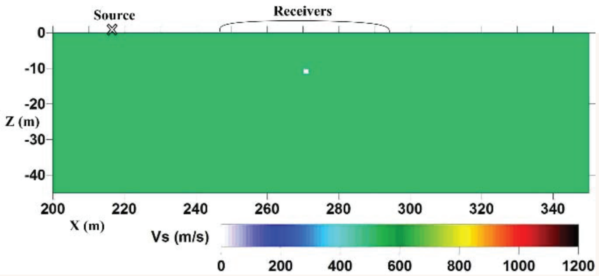

Figure 2. Shear-wave velocity model used for calculating synthetic seismic shot records showing the location of the void (the white square), source (cross), and receivers.

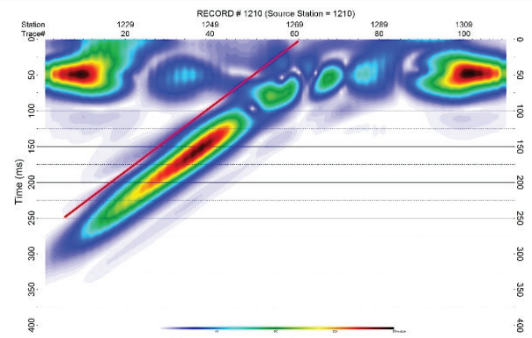

Figure 3. 2-D backscatter section displayed in instantaneous amplitude from a model with a void located at station 1270 and a red line pointing to it following the backscatter energy trend.

For data processing convenience, the left edge of the void was assigned to the station number 1270 (a horizontal location number) corresponding to x = 270 m (Figure 2). Backscatters can be identified on shot records as seismic events originating from the surface-wave energy trend at the horizontal location of an anomalous object (e.g., fault, boulder, void) and having a slope in a direction opposite to that of the source-generated surface wave (Figure 1). Record 5019 (Figure 1) is calculated using source and receiver locations indicated on the seismic model (Figure 2Figure 1).

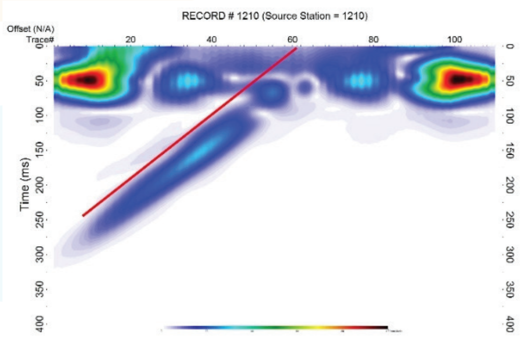

Figure 4. 2-D backscatter section displayed in instantaneous amplitude from a model with a boulder located at station 1270 and a red line pointing to it following the backscatter energy trend.

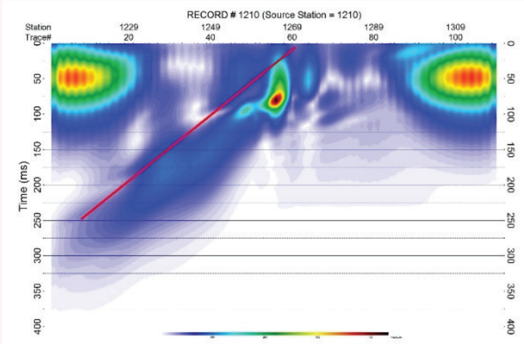

Figure 5. 2-D IA-BASW results displayed in instantaneous amplitude from a model with a void located at station 1270 and a red line pointing to it following the backscatter energy trend.

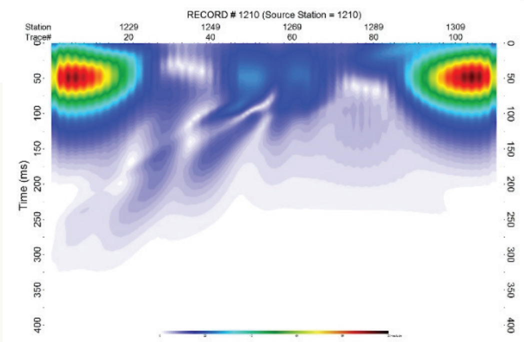

Figure 6. 2-D IA-BASW results displayed in instantaneous amplitude from a model with a boulder located at station 1270 and a red line pointing to it.

BASW of the two models provided backscatter sections that were very similar, with the void model having stronger backscatter energy originating at station 1270 (Figure 3) when compared to the boulder model (Figure 4). Such a minor difference did not appear sufficient for using it as a criteria on real data.

However, entering the instantaneous amplitudes from the two models into the BASW processing flow (IA-BASW) resulted in images that had a different backscatter response from station 1270. The IA-BASW backscatter response from the void (Figure 5) was weaker than the response from the BASW alone (Figure 3) but the linear energy trend could still be identified. However, the IA-BASW scatter from the boulder (Figure 6) had a different pattern, significantly weaker, with little or no linear trend in comparison to those from the void (Figure 5) and from the conventional BASW analysis (Figure 4). We hypothesized that such negligible signature has the potential to help discriminate voids in the presence of multiples scatters on conventional BASW images obtained from real-world data.

Real Tunnel Data

Data were acquired over a test tunnel in an arid desert environment in southern Arizona. Based on lithologic information recorded during drilling of shallow boreholes at this site, the near surface (upper 30 m) is composed of predominantly loose to dense clayey sands and hard sandy clays. The 9.2 m deep, 96 m long, 1.3 x 2.0 m air-filled tunnel was constructed using methods similar to clandestine tunnel construction along the US-Mexico border—i.e. a large trench was not cut and backfilled during construction, therefore, maintaining the in situ geophysical properties of the overlying and surrounding sediment (Sloan et al., 2015; Peterie et al., 2016). The seismic source was a rubber band assisted weight drop (RAWD) 36 m off-end from the line of twenty-four seismic receivers towed in a land streamer (Ivanov et al., 2006). Receivers were 4.5 Hz vertical geophones spaced at 1.22 m intervals. Five shots were fired and recorded separately at each source station. Source and receivers advanced by two stations in a roll-along approach, occupying a total of 62 source stations with 177 m of active receiver coverage. The seismic line was oriented perpendicular to the tunnel, intersecting the tunnel at station 1058.

We processed the data using KGSSeisUtilities software developed by the Kansas Geological Survey.

The conventional BASW image (Figure 7) revealed many backscatter events, including one from a known tunnel location (station 1058). While the tunnel produced the strongest backscatter feature, it would be difficult to separate it from other scatters without a-priori knowledge from at least three more backscatter events of interest, such as those converging to stations 962, 1025, and 1050. The IA-BASW backscatter image (Figure 8) had a weak linear event originating from the known location of the tunnel (station 1058) that is hardly noticeable. However, there were fewer linear events in comparison to Figure 5 as expected from the model tests with these being difficult to discern. Furthermore, when the conventional BASW section was combined with the IA-BASW section the tunnel response was enhanced. There were fewer backscatter anomalies and an improved elongated appearance and horizontal resolution of the backscatter from the tunnel.

Figure 7. 2-D BASW results displayed in instantaneous amplitude with the tunnel located below station 1058. The red line indicates a liner energy trend intercepting time = 0 at station 1058.

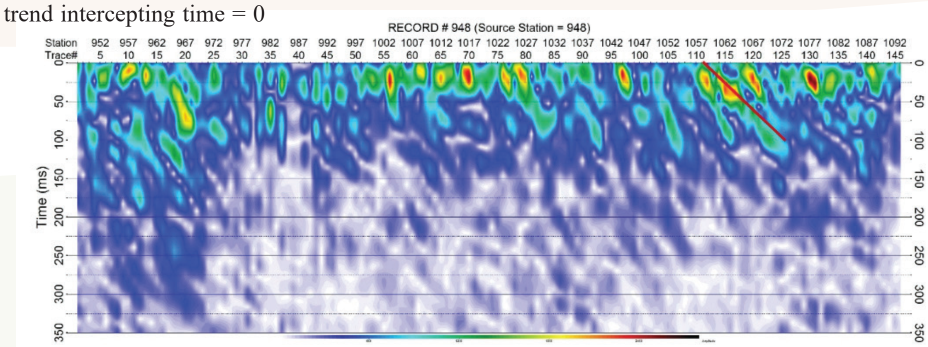

Figure 8. 2-D IA-BASW results displayed in instantaneous amplitude with the tunnel located at station 1058. The red line indicates a liner energy trend intercepting time = 0 at station 1058.

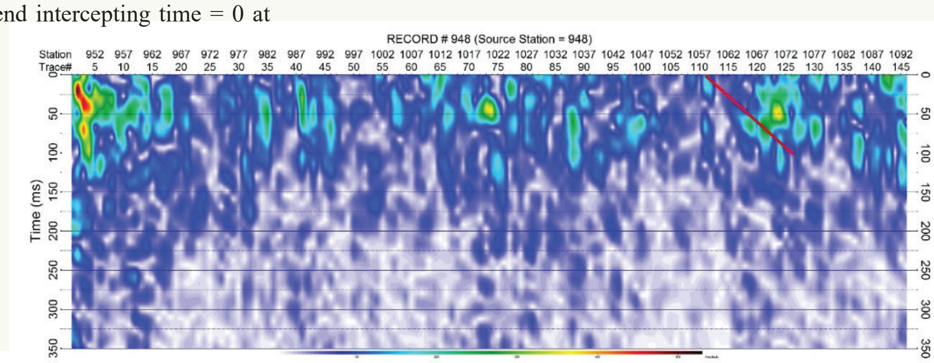

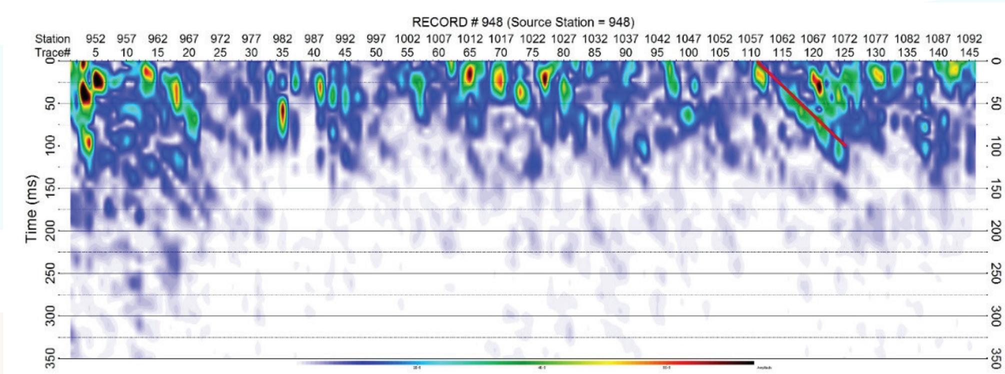

Figure 7. 2-D BASW – IA-BASW results displayed in instantaneous amplitude with the tunnel located at station 1058. The red line indicates a liner energy trend intercepting time = 0 at station 1058.

While it is difficult to precisely identify its location on the BASW-only image between stations1057 and 1060 (Figure 7), it is clearly notable on the combined image with a distinct linear backscatter trend originating from station 1058 (Figure 7), which is the true location of the tunnel.

Conclusions

Using instantaneous amplitudes as input to the backscatter processing flow appears to suppress surface-wave backscatters from geologic heterogeneities. Such an approach can help reduce the number of anomalies that could potentially be interpreted as voids. Thus it can be considered an additional tool for BASW.

The ability to observe even a weak linear event from a known tunnel location in the practical absence of other linear events on the IA-BASW section, encourages us to continue our research into data conditioning to improve the IA-BASW approach.

Acknowledgments

We are thankful to our field crew for the help with data acquisition. We also appreciate Mary Brohammer for her assistance in manuscript preparation.

References

Blonk, B., and G. C. Herman, 1994, Inverse Scattering of Surface-Waves - a New Look at Surface Consistency: Geophysics, 59, 963-972.

Grandjean, G., and D. Leparoux, 2004, The potential of seismic methods for detecting cavities and buried objects: experimentation at a test site: Journal of Applied Geophysics, 56, 93-106.

Herman, G. C., P. A. Milligan, Q. C. Dong, and J. W. Rector, 2000, Analysis and removal of multiply scattered tube waves: Geophysics, 65, 745-754.

Ivanov, J., R. D. Miller, P. Lacombe, C. D. Johnson, and J. W. Lane, 2006, Delineating a shallow fault zone and dipping bedrock strata using multichannal analysis of surface waves with a land streamer: Geophysics, 71, A39-A42.

Ivanov, J., R. Miller, and S. Peterie, 2016, Detecting and delineating voids and mines using surface-wave methods in Galena, Kansas, SEG Technical Program Expanded Abstracts 2016, 2344-2350.

Luke, B., and C. Calderón-Macías, 2008, Scattering of surface waves due to shallow heterogeneities, SEG Technical Program Expanded Abstracts 2008, 1283-1287.

Nasseri-Moghaddam, A., G. Cascante, C. Phillips, and D. J. Hutchinson, 2007, Effects of underground cavities on Rayleigh waves - Field and numerical experiments: Soil Dynamics and Earthquake Engineering, 27, 300-313.

Park, C., R. Miller, and J. Xia, 1998, Ground roll as a tool to image near-surface anomaly, 68th Annual International Meeting, SEG, Expanded Abstracts, 874-877.

Park, C., R. Miller, and J. Ivanov, 2002, Filtering Surface Waves, Symposium on the Application of Geophysics to Engineering and Environmental Problems 2002, SEI9-SEI9.

Schwenk, J. T., S. D. Sloan, J. Ivanov, and R. D. Miller, 2016, Surface-wave methods for anomaly detection: Geophysics, 81, EN29-EN42.

Sloan, S. D., S. L. Peterie, J. Ivanov, R. D. Miller, and J. R. McKenna, 2010, Void detection using near-surface seismic methods, in R. D. Miller, J. D. Bradford and K. Holliger, eds., Advances in Near-Surface Seismology and Ground-Penetrating Radar: Tulsa, Society of Exploration Geophysicists, SEG Geophysical Developments 201-218.

Sloan, S. D., S. L. Peterie, R. D. Miller, J. Ivanov, J. T. Schwenk, and J. R. McKenna, 2015, Detecting clandestine tunnels using near-surface seismic techniques: Geophysics, 80, EN127-EN135.

Snieder, R., 1986, 3-D Linearized Scattering of Surface-Waves and a Formalism for Surface-Wave Holography: Geophysical Journal of the Royal Astronomical Society, 84, 581-605.

Zeng, C., J. H. Xia, R. D. Miller, and G. P. Tsoflias, 2011, Application of the multiaxial perfectly matched layer (M-PML) to near-surface seismic modeling with Rayleigh waves: Geophysics, 76, T43-T52.